

Paper

Analysis of a Modified Half-Bridge Type Inverter for Improvement of Power Factor and Harmonic Distortion

Hirofumi MATSUO, Fujio KUROKAWA, Tsutomu KITAJIMA and Lishau TU

Dept. of Elect. Eng. & Comp. Sci. Nagasaki University Nagasaki, 852, Japan

Keiichi SHIMIZU

Toshiba Lighting & Tech. Corp. Kanagawa, 237 Japan

Received Dec. 17, 1997

ABSTRACT

This paper deals with the analysis of a novel modified half-bridge type inverter for electronic ballast of fluorescent lamps, in which the functions of the active filter and inverter are combined, and the power factor and harmonic distortion in the input current are improved sufficiently. After discussing, the equivalent circuit model and the operation mode of the proposed half-bridge type inverter, we proceed to analyze its performance characteristics theoretically and experimentally. As a result, it is clarified that the new modified half-bridge type inverter has excellent characteristics such as high power factor over 0.97, low total harmonic distortion factor less than 11.3%, high power efficiency of 92% and low crest factor of 1.56.

1. Introduction

Recently, the electronic ballast for fluorescent lamps is required to satisfy the maximum limit of IEC 1000-3-2 Class C with regard to the input current harmonics[1]-[4]. The active filter method has been often employed to reduce the input current distortion in the electric and electronic power systems. However, due to the cascade connection of the ac-dc converter and inverter, this method has the defects such as the complicated circuit configuration, high cost, large size, low power efficiency and so forth.

The purpose of this paper is to present a novel modified half-bridge type inverter for the electronic ballast of fluorescent lamps[5],[6], in which the functions of the active filter and inverter are combined, and to examine its performance characteristics. The proposed inverter is fundamentally composed of the resonant type half-bridge inverter[7]-[10]. After discussing the equivalent circuit model and the operation mode of the proposed inverter in detail to clarify the fundamental operation principle, we proceed to analyze the performance characteristics such as the power factor and harmonic distortion of the input current, and crest factor of the output voltage theoretically and experimentally.

2. Circuit Configuration, Equivalent Circuit Model and Operation Mode

Fig.1 shows a new modified half-bridge type inverter for the electronic ballast of fluorescent lamps, in which the functions of active filter and inverter are combined. This circuit is composed of the ac power source e_{ac} , input noise filter of an inductor L_F , capacitors C_{F1} and C_{F2} , bridge rectifier of diodes D_{B1} , D_{B2} , D_{B3} and D_{B4} , two main switches

T_{r1} and T_{r2} connected reversely in parallel with diodes D_1 and D_2 , transformer T , smoothing capacitor C_1 , resonant capacitor C_2 , pre-heat capacitor C_o and fluorescent lamp as a load. In Fig.1, i_{ac} is the ac input current, and i_{acB} and i_B are the input and output currents of the diode bridge, respectively. i_{S1} , i_{S2} , i_L , i_{C1} and i_{C2} are the currents through the antiparallel connection of T_{r1} and D_1 , that of T_{r2} and D_2 , primary winding of T , C_1 and C_2 , respectively. V_{S1} , V_{S2} , V_L , V_{C1} and V_{C2} are the voltages across T_{r1} , T_{r2} , primary winding of T , C_1 and C_2 , respectively. e_o is the ac output voltage. The inverter in Fig.1 has remarkable features as follows: (i) The capacitor C_1 has large capacitance ($C_1=270\mu F$) to keep the crest factor small. The capacitor C_2 has extremely small capacitance ($C_2=0.027\mu F$) to prevent the input rush current and to work as a resonant capacitor. (ii) The coupling of the primary and secondary windings of the transformer T is loose enough to give a relatively large leakage inductance between those two windings. (iii) The capacitors C_2 and C_o , exciting inductor and leakage inductor of transformer T constitute a resonant circuit.

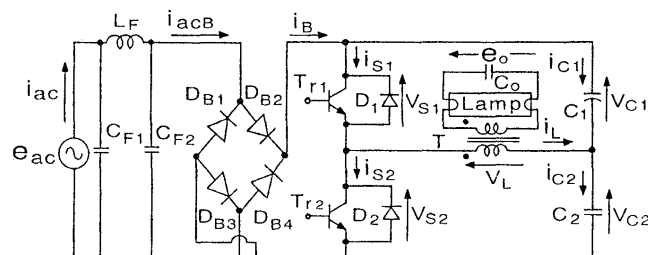


Fig. 1 Basic circuit configuration of the new modified half-bridge type inverter for the electronic ballast of fluorescent lamps.

The following assumptions are made for the simplification of the circuit analysis:

- 1) The switches T_{r1} and T_{r2} , and the diodes D_1 and D_2 have the ideal switching characteristics. Therefore, the ideal switches S_1 and S_2 are employed instead of the antiparallel connection of T_{r1} and D_1 and that of T_{r2} and D_2 , respectively.
- 2) Each circuit element is ideal and has no power loss.
- 3) The diode D_B is used instead of the rectifier diodes D_{B1} , D_{B2} , D_{B3} and D_{B4} .
- 4) The number of turns of transformer T is normalized and is equal to unity. Also, the transformer T has exciting inductance L_e and leakage inductance L_ℓ . These inductors have the linear magnetizing characteristics.
- 5) The capacitance of C_1 is so large that C_1 can be replaced by a constant voltage source E_{C1} .
- 6) The resistance of fluorescent lamp is constant in the steady-state. Therefore, the lamp can be replaced by a constant resistor R.
- 7) The noise filter is neglected because it is used to reduce the high frequency current ripple and does not affect the circuit operation of the inverter.
- 8) Since the ac input voltage e_{ac} is rectified by the bridge rectifier diode and the frequency of the commercial ac line is lower enough than the switching frequency of the inverter, e_{ac} is replaced by the a constant voltage source E_{ac} .

Taking the above assumptions into consideration, the inverter shown in Fig.1 is represented by the simplified equivalent circuit shown in Fig.2. In this figure, e_o^* , C_o^* and R^* denote the values of e_o , C_o and R normalized by the number of turns of the transformer T, respectively. i_L , i_{Lc} and i_o^* are the current through L_ℓ , L_e and R^* , respectively. Fig.3 shows the typical waveforms of the driving base currents i_{b1} and i_{b2} of T_{r1} and T_{r2} , respectively, Voltage V_{S1} and current i_{S1} of S_1 , and voltage V_{S2} and current i_{S2} of S_2 in Fig.1 or Fig.2. The phase difference between i_{b1} and i_{b2} are 180 degrees.

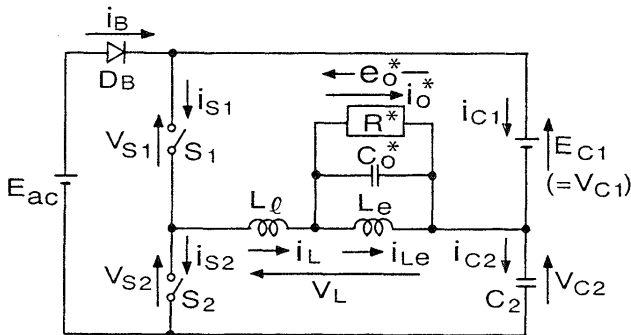


Fig. 2 Simplified equivalent circuit of Fig.1.

It is seen in Fig.3 that there can not exist the state in which S_1 and S_2 are on or off simultaneously because the on

and off operations of S_1 and S_2 are repeated alternately, and that the zero current switching(ZCS) operations of S_1 and S_2 are achieved.

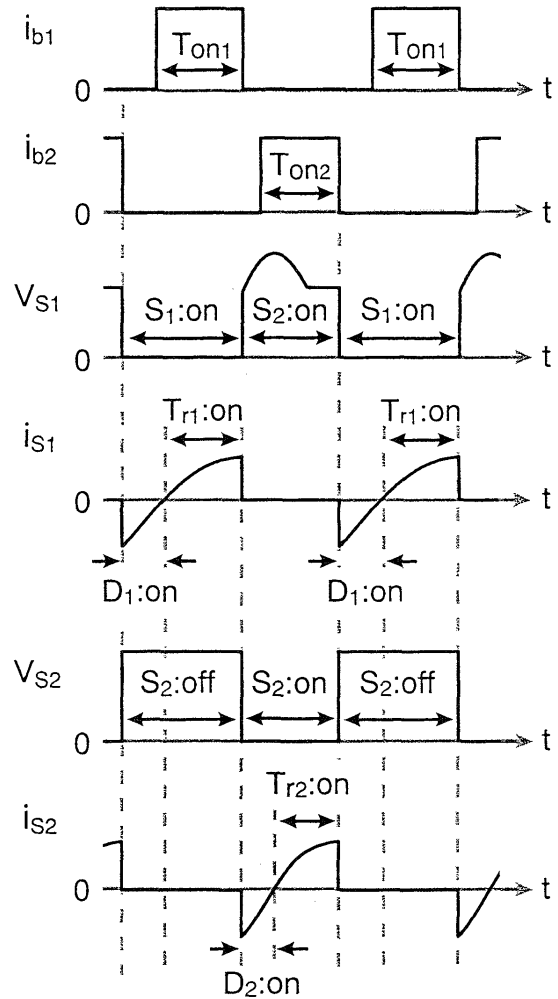


Fig. 3 Typical waveforms of the driving base currents i_{b1} and i_{b2} of T_{r1} and T_{r2} , respectively, voltage V_{S1} and current i_{S1} of S_1 , and voltage V_{S2} and current i_{S2} of S_2 in Fig.1 or Fig.2.

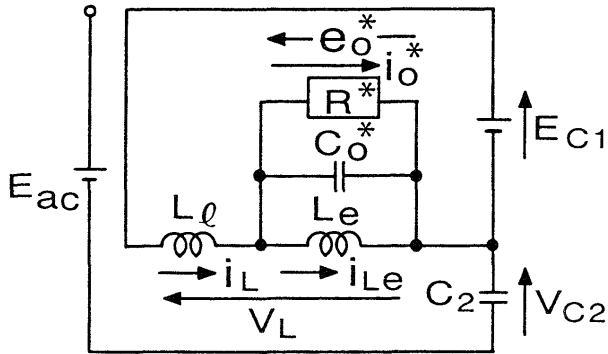
Also, there can not exist the state in which S_2 and D_B are off and on, respectively, at the same time because V_{C2} across C_2 is clamped at the constant value of $E_{ac} - E_{C1}$, i_{C2} can not flow through C_2 , i_B is equal to i_{C2} in that state and consequently i_B can not flow through D_B . From the above discussion, only three states out of eight ($=2^3$) ones in the circuit of Fig.2 have the physical meaning. Therefore, the circuit of Fig.2 is divided into three states of behavior according to the combinations of the on and off conditions of the switches S_1 and S_2 , and diode D_B , which are shown in Table 1. Figs.4 (a), (b) and (c) show the equivalent circuits of states 1, 2 and 3 in Table 1, respectively. Taking account of the states in Table 1 and the transition condition of these states, it is derived that there exist two operation modes Mode I and Mode II as shown in Table 2.

Table 1 States of behavior.

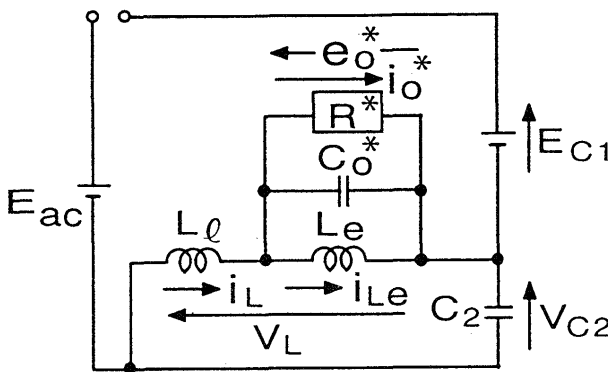
State	S ₁	S ₂	D _B
1	On	off	off
2	off	On	off
3	off	On	On

Table 2 Operation modes.

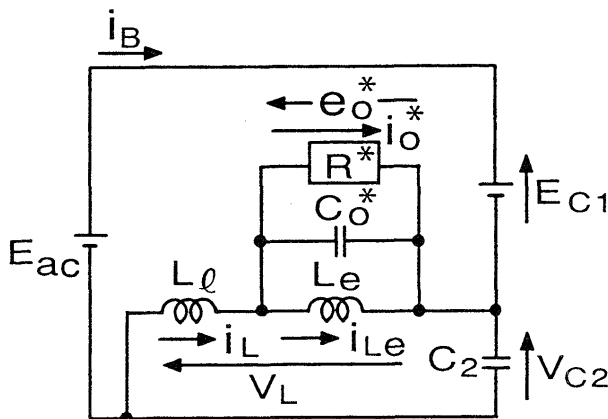
Mode	State Sequences
I	1 → 2
II	1 → 2 → 3



(a)



(b)



(c)

Fig. 4 Equivalent circuits. (a) State 1 (b) State 2 (c) State 3

By using the equivalent circuits shown in Fig.4, the circuit operation is explained as follows:

state 1

The switch S₁ is on, and the switch S₂ and diode D_B are off. This state appears after the switch S₂ is turned off. i_L flows through the path of E_{C1}, L_ℓ and the parallel circuit of L_e, C_o^{*} and R^{*}. In this state, i_B(=i_{ac}) does not flow. The output consumption energy is supplied by E_{C1}.

From Fig.4(a),

$$E_{C1} = L_{\ell} \frac{di_L(t)}{dt} + L_e \frac{di_{Le}(t)}{dt} \quad (1)$$

$$e_o^*(t) = R^* i_o^*(t) \quad (2)$$

$$e_o^*(t) = L_e \frac{di_{Le}(t)}{dt} \quad (3)$$

$$C_o^* \frac{de_o^*(t)}{dt} = i_L(t) - i_{Le}(t) - i_o^*(t) \quad (4)$$

$$V_L = E_{C1} + (V_{C1}(t)) \quad (5)$$

$$V_{C2}(t) = V_{C2}^{(0)} \quad (6)$$

$$V_{S2}(t) = E_{C1} + V_{C2}(t) \quad (7)$$

$$i_{S1}(t) = i_L(t) \quad (8)$$

$$i_{C2}(t) = 0 \quad (9)$$

$$V_{S1}(t) = 0 \quad (10)$$

$$i_B(t) = 0 \quad (11)$$

where V_{C2}(0) is the initial voltage of the capacitor C₂.

state 2

The switch S₂ is on. The switch S₁ and diode D_B are off. This state appears after the switch S₁ is turned off and S₂ is turned on. The resonant current flows through the path of L_ℓ, the parallel circuit of L_e/C_o^{*}//R^{*}, and C₂. In this state, i_B(=i_{ac}) does not flow.

From Fig.4 (b),

$$i_L(t) = C_2 \frac{dv_{C2}(t)}{dt} \quad (12)$$

$$V_{C2}(t) + V_L(t) = 0 \quad (13)$$

$$V_L(t) = L_{\ell} \frac{di_L(t)}{dt} + e_o^*(t) \quad (14)$$

$$e_o^*(t) = R^* i_o^*(t) \quad (15)$$

$$e_o^*(t) = L_e \frac{di_{Le}(t)}{dt} \quad (16)$$

$$C_o^* \frac{de_o^*(t)}{dt} = i_L(t) - i_{Le}(t) - i_o^*(t) \quad (17)$$

$$V_{s1}(t) = E_{C1} - V_L(t) \tag{18}$$

$$\dot{i}_{s2}(t) = -i_L(t) \tag{19}$$

$$\dot{i}_{s1}(t) = 0 \tag{20}$$

$$V_{s2}(t) = 0 \tag{21}$$

$$\dot{i}_B(t) = 0 \tag{22}$$

state 3

The switch S_2 and diode D_B are on, and the switch S_1 is off. This state appears after E_{ac} becomes larger than $E_{C1} + V_{C2}$ and S_2 is turned-on. Therefore, in this state, $i_b (= i_{i_{ac}})$ flows through the path of E_{ac} , D_B , E_{C1} , the resonant and output circuits of L_ℓ , C_2 and $L_c // C_o^* // R^*$.

From Fig.4(c),

$$E_{C1} = E_{ac} = L_\ell \frac{di_L(t)}{dt} + e_o^*(t) \tag{23}$$

$$e_o^*(t) = R^* i_o^*(t) \tag{24}$$

$$e_o^*(t) = L_e \frac{di_L(t)}{dt} \tag{25}$$

$$C_o^* \frac{de_o^*(t)}{dt} = i_L(t) - i_{Lc}(t) - i_o^*(t) \tag{26}$$

$$V_{C2}(t) = E_{ac} - E_{C1} \tag{27}$$

$$V_{S1}(t) = E_{ac} \tag{28}$$

$$\dot{i}_{s2}(t) = -i_L(t) \tag{29}$$

$$i_B(t) = -i_L(t) \tag{30}$$

$$i_{C2}(t) = 0 \tag{31}$$

$$i_{S1}(t) = 0 \tag{32}$$

$$V_{S2}(t) = 0 \tag{33}$$

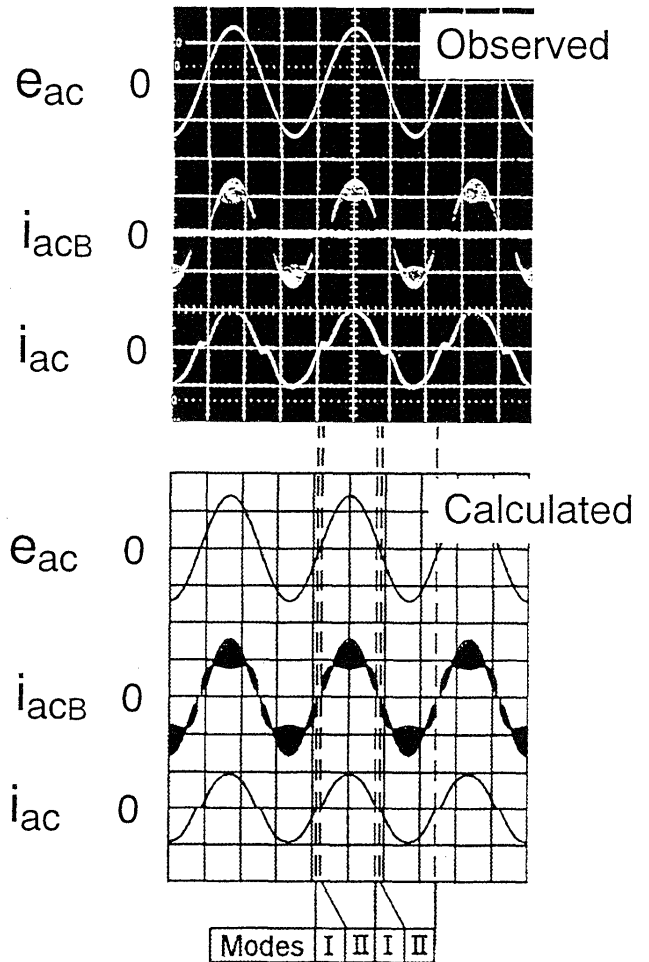
where $i_b(t) = |i_{i_{ac}}(t)|$.

In state3, the energy stored in L_ℓ and L_c in state 2 charges the voltage source E_{C1} as a boost energy together with E_{ac} . Therefore, the operations in states 2 and 3 play a role as an active filter and that in state 1 does as a half-bridge inverter.

3. Performance Characteristics

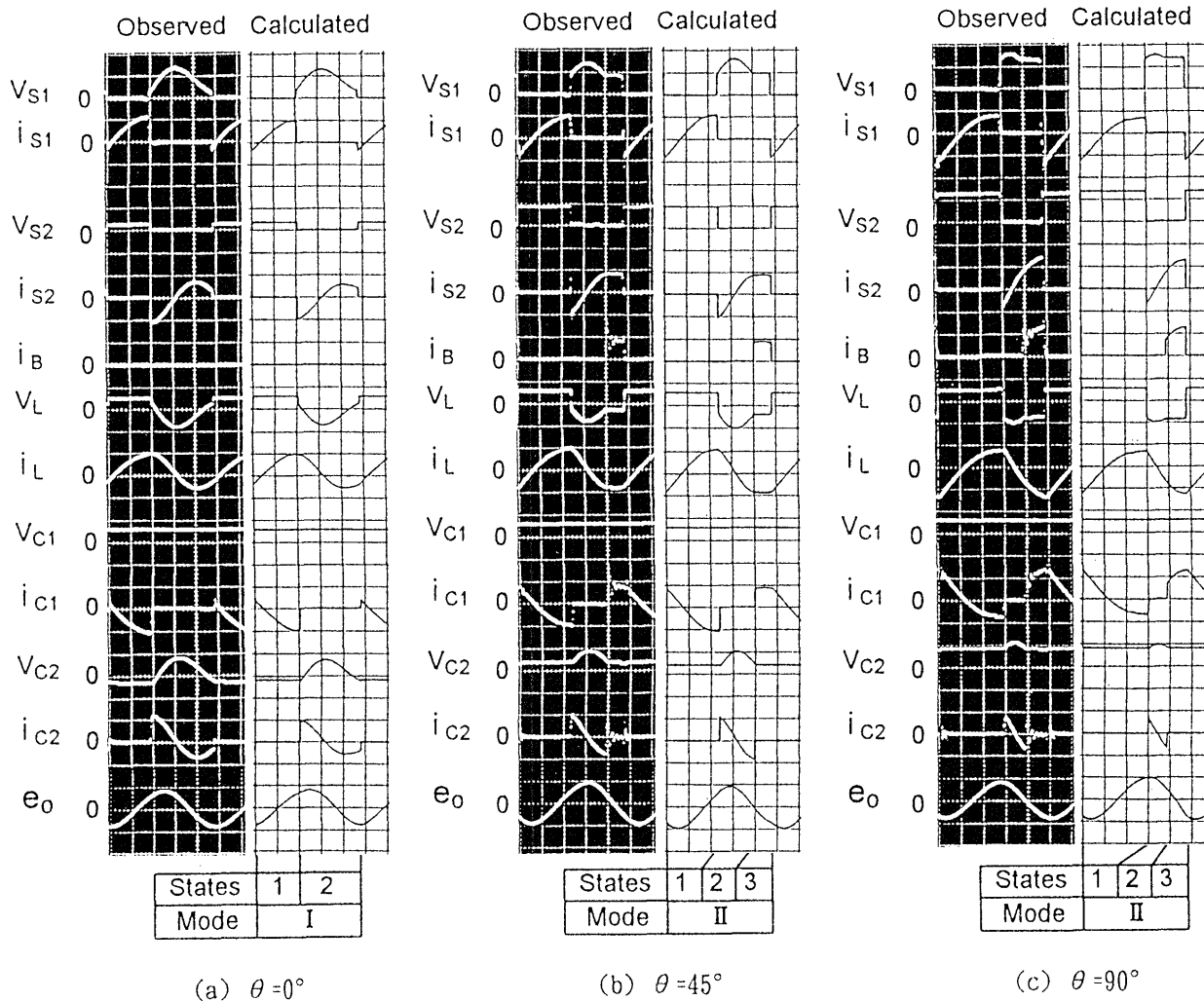
Figs.5 (a), (b) and (c) show the observed and calculated waveforms of the voltages and currents of the circuit elements in Fig.1, corresponding to the phases at $\theta=0^\circ$, 45° and 90° of the ac input voltage e_{ac} . In these figures, taking account of the analytical results in each operation

mode and the energy balance relation[11] among the input and output energies, and energy of E_{C1} during the one switching period T_s of inverter and a half period of the commercial ac line frequency f_{ac} , the calculated results are derived. The circuit parameters are $e_{ac}=200V$, $f_{ac}=60Hz$, $f_s \cong 52kHz$, $L_c=0.33mH$, $L_\ell=0.36mH$, $C_1=270\mu F$, $C_2=0.027\mu F$, $C_o=5600pF$, $R=1200\Omega$ and turn ratio of primary and secondary windings of the transformer T is 71:169. $C_{F1}=0.22\mu F$, $C_{F2}=0.68\mu F$ and $L_r=0.33mH$. The on-time intervals T_{on1} and T_{on2} of the main switches T_{r1} and T_{r2} in Fig.3, respectively, are fixed to be 7.5 μs . T_{r1} and T_{r2} are driven and controlled by the self-oscillator. The detailed discussion of the control of T_{r1} and T_{r2} is omitted in this paper. It is seen in these figures that the calculated results agree well with the experimental ones and that the input current $i_b (\cong i_{i_{ac}})$ dose not flow in Mode I.



Horizontal : 5msec./div.
 Vertical : e_{ac} ; 200V/div.
 i_{acB}, i_{ac} ; 2A/div.

Fig. 6 Observed and calculated waveforms of the ac input voltage e_{ac} , input current of rectifier diode i_{acB} and ac input current i_{ac} .



Horizontal: $4\mu\text{sec./div.}$
 Vertical: $V_{s1}, V_{s2}, V_L, V_{C1}, V_{C2}$; 200V/div.
 e_o ; 400V/div.
 $i_{s1}, i_{s2}, i_B, i_L, i_{C1}, i_{C2}$; 2A/div.

Fig. 5 Observed and calculated waveforms of the voltages and currents of the circuit elements in Fig.1, corresponding to the phase at $\theta=0^\circ, 45^\circ$ and 90° of e_{ac} . (a) $\theta=0^\circ$ (b) $\theta=45^\circ$ (c) $\theta=90^\circ$

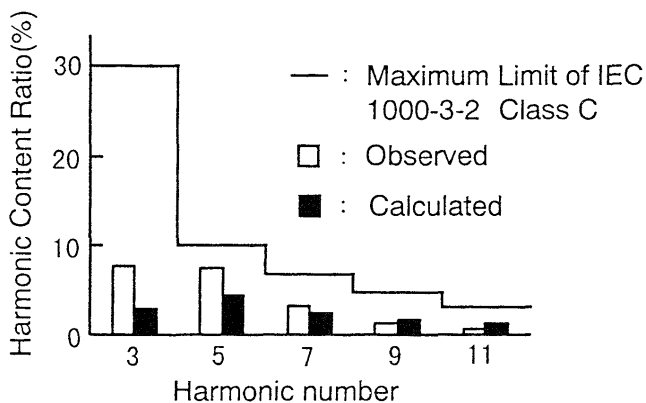


Fig. 7 Harmonic currents of i_{ac} .

Fig.6 shows the observed and calculated waveforms of the ac input voltage e_{ac} , input current i_{acB} of the rectifier diode and ac input current i_{ac} . The circuit parameters and variables of the inverter are the same as in Fig.5. The proposed inverter operates in Mode I in the neighborhood of the zero-cross point of e_{ac} and in Mode II at the relatively large value of e_{ac} , which are shown in Fig.6. In this case, the power factor is over 0.97 and input current total harmonic distortion factor is less than 11.3%.

Fig.7 shows the harmonic currents of i_{ac} . The circuit parameters are the same as in Fig.5. It is seen in this figure that the limitation of harmonic currents in IEC 1000-3-2 Class C is satisfied enough.

Fig.8 shows the observed and calculated waveforms of the output voltage e_o , corresponding to Fig.6. It is clarified

in this figure that the calculated result agrees well with the observed waveform, and that the crest factor is 1.56 and is within 1.7 of the maximum limit of IEC.

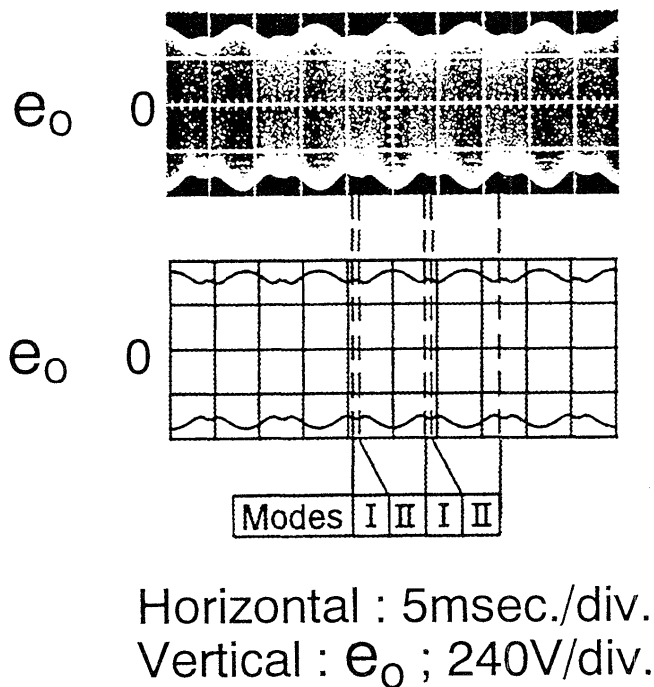


Fig. 8 Observed and calculated waveforms of the output voltage e_o .

4. Conclusion

The novel modified half-bridge type inverter for the electronics ballast of fluorescent lamps has been proposed and its performance characteristics have been examined theoretically and experimentally. The conclusions are as follows:

- 1) The operation of the proposed inverter is divided into three states of behavior, and there exist two operation modes by combining the above three states.
- 2) The proposed inverter can achieve high power factor over 0.97, low total harmonic distortion factor less than 11.3% and low crest factor of 1.56.
- 3) The maximum limits of harmonic currents in IEC 1000-3-2 Class C is satisfied by the proposed circuit. Moreover, high power efficiency of 92% can be achieved.

The design oriented analysis of the proposed circuit and control of the main switches are being studied and will be reported in a separate paper.

This work was supported in part by the 1997 Research and Education Grant-in-Aid of the Illuminating Engineering Institute of Japan.

References

- [1] N. Aoike, H. Matsuo and F. Kurokawa : "Trend of inverter technologies for operating gas discharge lamps," Technical Report of IEICE Japan, no. PE95-1, May 1995.
- [2] H. Matsuo, N. Aoike and F. Kurokawa : "A new combined voltage-resonant inverter with high power factor and low distortion factor," IEEE Power Electronics Specialists Conference Record, pp. 331-335, June 1994.
- [3] F. Kurokawa, N. Aoike, A. Hisako, H. Xu and H. Matsuo : "Improvement of performance characteristics of the combined voltage-resonant inverter," Proceedings of International Power Electronics Conference, pp. 1272-1277, April 1995.
- [4] H. Matsuo, F. Kurokawa, N. Aoike and H. Xu : "Performance characteristics of the combined voltage-resonant inverter," IEEE Power Electronics Specialists Conference Record, pp. 1159-1164, June 1995.
- [5] Y. Kitamura, K. Uratani, T. Kakitani and K. Shimizu: "Fluorescent lamp inverter with reduced harmonics," Technical Report of IEIE, vol. 13, no. B-11, Sep. 1995.
- [6] Y. Kitamura, K. Uratani, T. Kakitani and K. Shimizu: "Half-bridge type combined circuit with reduced harmonics," Proceedings of IEI Tokyo Chapter Annual Conference, vol. 25, no. 2, Oct. 1995.
- [7] F. C. Schwarz : "An improved method of resonant current pulse modulation for power converters," IEEE Trans. Ind. Electron. Contr. Instrum., vol. IECI-23, no. 2, pp. 971-978, May 1976.
- [8] S. Muroyama and K. Sakakibara: "An operating frequency range reduction method in a series resonant converter," Trans. IEICE Japan, vol. J68-B, no. 11, pp. 1235-1241, Nov. 1985.
- [9] I. E. Batarseh and C. Q. Lee : "Steady state analysis of the parallel resonant converter with LLC-type commutation network," IEEE Power Electronics Specialists Conference Record, pp. 971-978, June 1989.
- [10] M. Asano, H. Matsuo, F. Kurokawa and H. Mae : "Analysis of a half-bridge type series resonant dc-dc converter with auxiliary switches," Proceedings of European Conference on Power Electronics and Applications, pp. 2.618-2.623, June 1995.
- [11] H. Matsuo, H. Hayashi, F. Kurokawa and M. Asano : "A general analysis of the zero-voltage switched quasi-resonant buck-boost type dc-dc converter in the continuous and discontinuous modes of the reactor current," IEICE Trans. Communications, vol. E75-B, no. 11, pp. 1159-1170, Nov. 1992.